Supporting Information

Sulfur-Induced Structural and Electronic Engineering of Ru Nanoclusters for Highly Efficient Hydrogen Evolution

Xinyu Li,[a,b,‡] Jing Li,[a,‡] Jingwen Yin,[a] Guangyao Zhou,*[,c] Lei Chen,*[,a,b] Lin Xu[a] and Yawen Tang*[,a]

[a] Jiangsu Key Laboratory of New Power Batteries, Jiangsu Collaborative Innovation Center of Biomedical Functional Materials, School of Chemistry and Materials Science, Nanjing Normal University, Nanjing 210023, PR China

[b] Nanjing Yuqing Environmental Technology Co., Ltd, Nanjing 211500, PR China

[c] College of Science, Jinling Institute of Technology, Nanjing, 211169, PR China

‡ X. Li and J. Li contributed equally to this work.

Experimental section

Reagents and chemicals

Chemicals including melamine ($C_3H_6N_6$, AR, 99%), Cyanuric acid ($C_3H_3N_3O_3$, AR, 98%), Dimethyl sulfoxide (C_2H_6SO, AR, DMSO), Ammonia solution ($NH_3 \cdot H_2O$, 25-28%), Dopamine hydrochloride ($C_8H_{11}NO_2 \cdot HCl$, 98%, PDA) were purchased from Shanghai Aladdin Biochemical Technology Co., Ltd. Ruthenium (III) chloride hydrate ($RuCl_3 \cdot xH_2O$), commercial Pt/C (20 wt.% Pt) and Ru/C (15 wt.% Ru) catalyst were obtained from Johnson Matthey Chemicals Ltd. Nafion solution (5 wt.%), Potassium hydroxide (KOH, 90%), Acetone (AR), Methanol (CH_3OH, 99.5%) and Ethanol (C_2H_5OH, 99.7%) were purchased from Sinopharm Chemical Reagent Co., Ltd. All of the chemicals were used directly without further purification. Deionized water was used for all experiments.

Synthesis of MCDs

Dissolve 4 mmol of melamine in 20 ml of DMSO solution and label it as solution A. 4 mmol of cyanic acid was dissolved in 10 mL of DMSO solution and labeled as solution B. Then add the solution B into the solution A and ultrasound dissolves for an hour. The mixed dissolved solution was centrifugally washed three times and then dried at 30 ℃ to obtain MCDs.

Synthesis of Ru-PDA@MCDs and Ru@S, N-CMFs

Dissolve 300 mg MCDs in 100 mL deionized water, and add 0.25 mL $NH_3 \cdot H_2O$, 150 mg PDA and 20 mg $RuCl_3 \cdot xH_2O$ after ultrasonic dissolution. After the completion of reaction, the mixture solution was centrifuged and washed with deionized water and

absolute ethanol several times. The as-obtained samples were collected and then dried at 60 ℃ for 12 h, calling it Ru-PDA@MCDs. Ru-PDA@MCDs were pyrolyzed under Ar atmosphere in a tube furnace at 800 ℃ for 3 h with a heating rate of 3 ℃ min^{-1} to yield Ru@S, N-CMFs.

Physicochemical characterizations

Scanning electron microscopy (SEM) measurement was carried out on a Hitachi S5500 scanning electron microscope. The morphology of products was evaluated by transmission electron microscopy (TEM), high resolution transmission electron microscopy (HRTEM) and energy dispersive X-ray (EDX) mapping images were performed on a JEOL JEM-2010F transmission electron microscope with an accelerating voltage of 200 kV. The atomic phase characterization of the material is performed on annular dark field scanning transmission electron microscopy (AC HAADF-STEM) images. X-ray diffraction (XRD) patterns on a Model D/max-RC X-ray diffractometer with a Cu Kα radiation source (λ = 1.5406 Å) was employed to analyze the crystallinity of the samples. The Raman spectra were measured on a Raman spectrometer (Lab RAM HR800, λ = 514 nm). The Brunauer-Emmett-Teller (BET) isotherms were determined on Quadrasorb SI. X-ray photoelectron spectroscopy (XPS) and ultraviolet photoelectron spectroscopy (UPS) analyses were operated on a Thermo VG Scientific ESCALAB 250 spectrometer using Al Kα X-ray radiation and He I resonance lines (21.2 eV), respectively. The inductively coupled plasma optical emission spectrometry (ICP-OES) could be examined by Perkin Elmer AVIO200.

Electrochemical measurement

All the electrochemical tests were carried out on a CHI 760E electrochemical analyzer in a three-electrode configuration at room temperature. A glassy carbon electrode (GCE, d = 3 mm), a saturated calomel electrode (SCE) and a graphite rod were served as the working electrode, reference electrode and counter electrode, respectively. The catalyst ink was prepared by ultrasonically dispersing 5 mg of catalyst in 1.0 mL of ethanol solution (the volume ratio of water to ethanol is 3:1) for 30 mins. Subsequently, 10 μL of the catalyst ink was dropped onto the surface of polished GCE and then dried at 40 ℃. After that, 3 μL of Nafion (5 wt.%, Sigma-Aldrich) was dropped on the catalysts modified GCE surface and dried before electrochemical test. The HER measurement was evaluated by linear sweep voltammetry (LSV) corrected against Ohmic potential drop (*IR*) losses in N_2-saturated 1.0 M KOH solution at a scan rate of 5 mV s^{-1}. The electrochemical double-layer capacitances (C_{dl}) were determined by a series of CV tests (scan rate: 20, 40, 60, 80 and 100 mV s^{-1}). The stability measurements were investigated by continuous CV scanning 1000 cycles at a scan rate of 0.1 V s^{-1}. The chronopotentiometry measurement was conducted at an overpotential of 100 mV. All the potentials have been referenced to reversible hydrogen electrode (RHE) in this work. The equation of potential conversion from SCE to RHE described as follows: $E_{RHE} = E_{SCE} + 0.0591\ pH + 0.242$. The ECSA can be calculated using the capacitance (C_{dl}). The special capacitance of a standard value of 40 μF cm^{-2} was used in the following equation of the ECSA.

$$ECSA = \frac{C_{dl}}{40\ \mu F\ cm^{-2}\ per\ cm^2}$$

MEA fabrication and AEMWE measurements

Anion-exchange membrane water electrolyzers (AEMWE) featuring serpentine flow channels (effective area: 1×1 cm^2) were employed to evaluate the practical applicability of the Ru@S, N-CMFs electrocatalyst, utilizing a graphite plate as the cathode and a titanium (Ti) plate as the anode. The Sustainion X37-50 RT anion exchange membrane was activated via overnight immersion in a 1.0 M KOH solution. The cathode ink formulation comprised 10 mg of catalyst powder, 210 μL of deionized water, 1.69 mL of isopropanol, and 100 μL of ionomer solution (Dioxide Materials, Sustainion XA-9, 5 wt. % in ethanol) in both cases. The applied anode catalyst was the nickel foam (NF) loaded NiFe-LDH prepared by hydrothermally (1×1 cm^2). The Ru@S, N-CMFs electrocatalyst ink was uniformly deposited onto the carbon paper (CP) substrate, serving as the cathode porous current collector, using an airbrush spraying technique. The catalyst loading was maintained at approximately 2.0 mg cm^{-2}. A membrane with an active area of 1 × 1 cm^2 was assembled between the NiFe-LDH/NF anode and the Ru@S, N-CMFs/CP cathode. Viton gaskets with suitable thickness were also placed to prevent the liquid/gas from leaking. The torque applied to assemble the cell was 3 Nm. The AEMWE test was operated at 80 ℃ and 1.0 M KOH was employed as electrolytes with a flow rate of 30 mL/min. Polarization curves were obtained from 1.2 to 2.0 V at a stepwise rate of 0.02 V. The electricity cost can be calculated as following equation: $W = U * Q = \left(2F * N_{H_2}\right) = U * (2F * V_{H_2}/V_m)$, where U is the cell voltage; Q is the number of electrons transferred to generate hydrogen; F is the Faraday constant (96485 C/mol); N_{H2} is the number of moles of hydrogen produced by the electrolyzer; V_{H2} is

the volume of hydrogen generated by the electrolyzer; V_m is Molar volume of gas (22.414 L/mol).

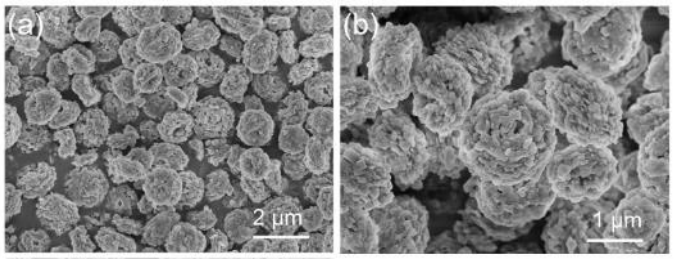

Figure S1. (a-b) SEM images of MCDs.

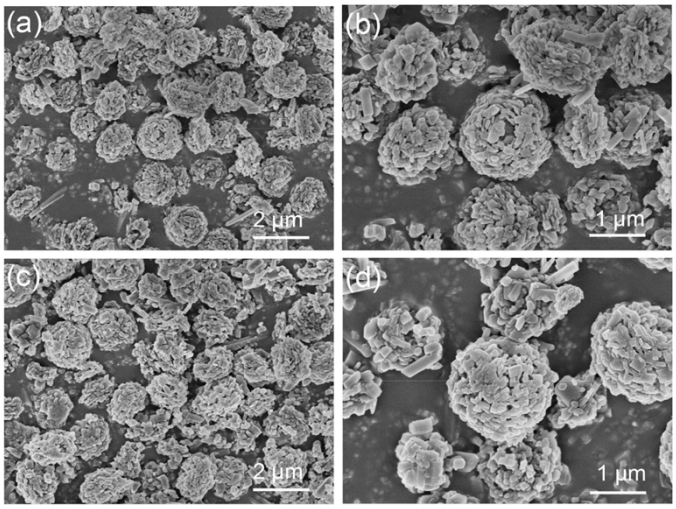

Figure S2. SEM images of MCDs, (a-b) synthesized at 60 ℃, and (c-d) synthesized at 0.1 M NaOH.

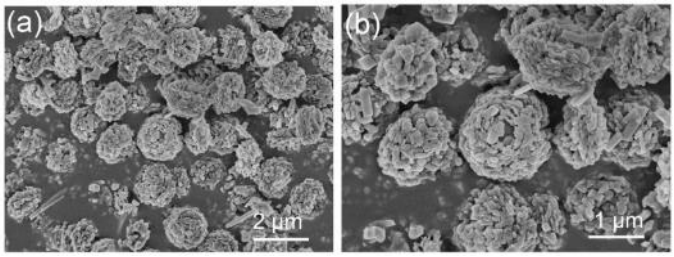

Figure S3. (a-b) SEM images of Ru-PDA@MCDs.

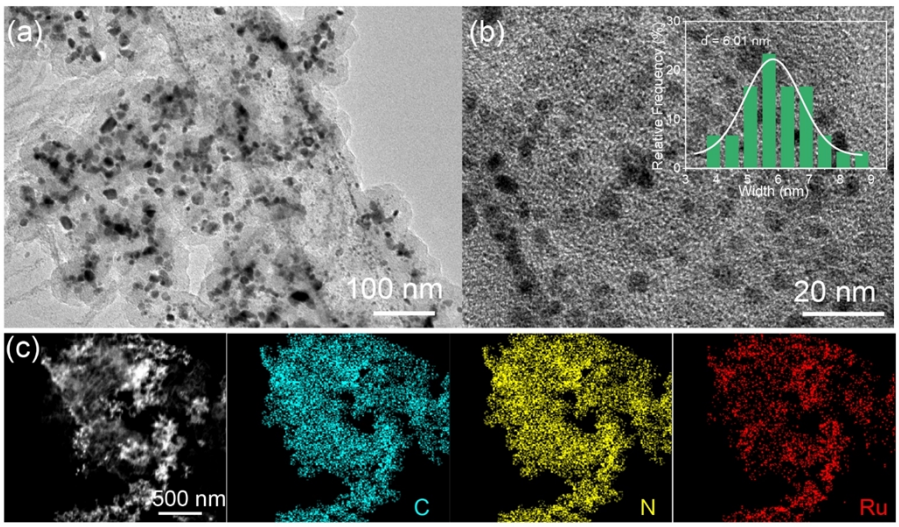

Figure S4. HRTEM images and mapping images of Ru@N-CMFs.

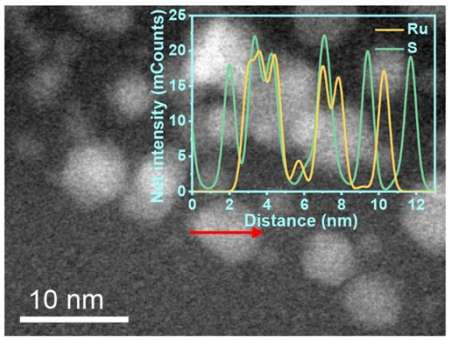

Figure S5. AC HAADF-STEM image of Ru@S, N-CMFs (inset EDX line scanning analysis of individual Ru nanoparticle).

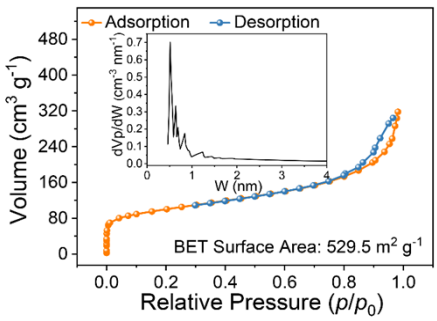

Figure S6. N_2 adsorption-desorption isotherms (inset: pore size distributions curve).

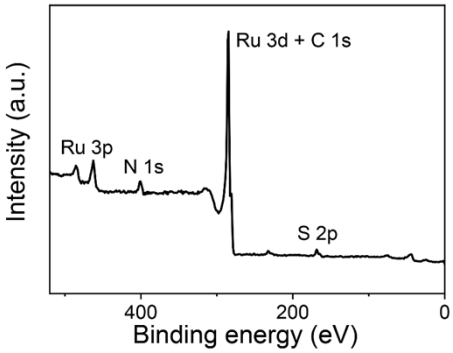

Figure S7. XPS survey spectra of Ru@S, N-CMFs.

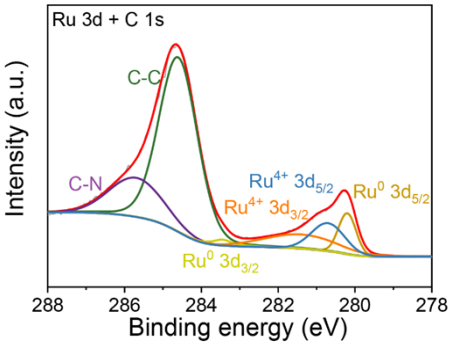

Figure S8. High-resolution Ru 3d + C 1s XPS spectrum of Ru@S, N-CMFs.

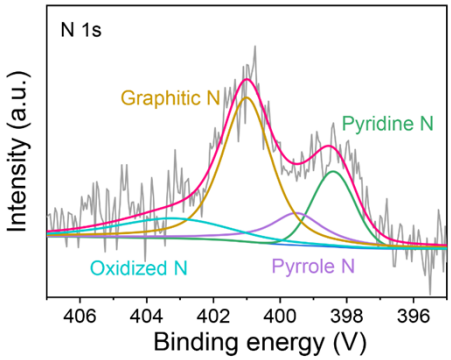

Figure S9. High-resolution N 1s XPS spectra of Ru@S, N-CMFs.

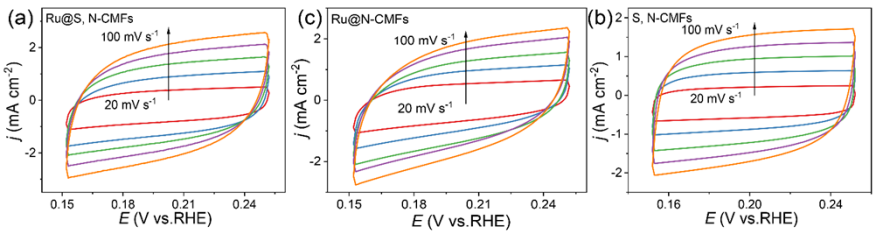

Figure S10. CV curves of (a) Ru@S, N-CMFs, (b) Ru@N-CMFs, and (c) S-CMFs.

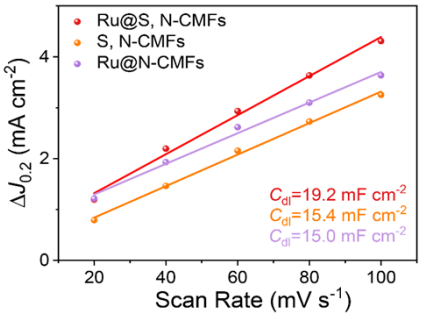

Figure S11. C_{dl} values of Ru@S, N-CMFs, Ru@N-CMFs and S-CMFs.

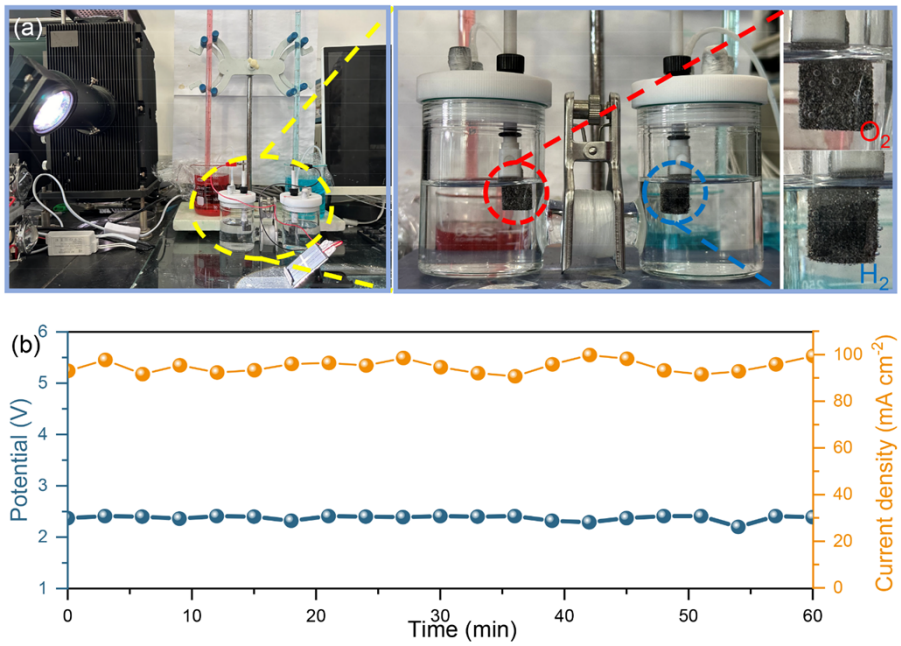

Figure S12. (a) digital photograph of a solar energy-driven H-type electrolyzer assembled by Ru@S, N-CMFs and RuO_2, (b) the voltage and generated current density of the solar cell during the daytime for water splitting.

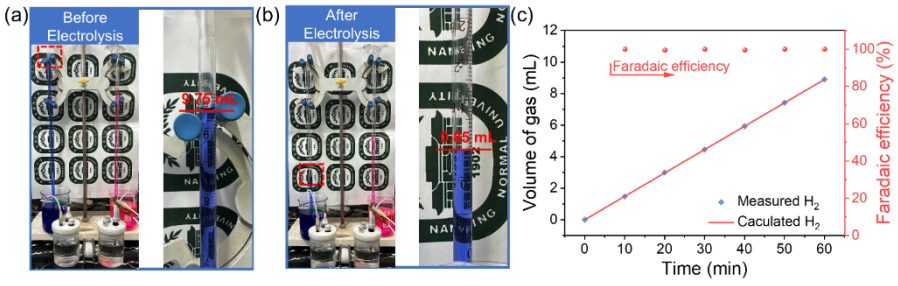

Figure S13. Faradaic efficiency test. (a)-(b) digital photographs of two-electrode electrolyzers before and after electrolysis, (c) experimental and theoretical yields of H_2 gas and Faradaic efficiency of the Ru@S, N-CMFs sample during water electrolysis at 20 mA cm^{-2} for 1 h.

Table S1. The Ru content of Ru@S, N-CMFs measured by inductively coupled plasma atomic emission spectroscopy (ICP-AES).

Sample	Ru content (wt.%)
Ru@S, N-CMFs	6.7558%

Table S2. Comparisons of HER activity of Ru@S, N-CMFs with some previously reported Ru-based catalysts in 1.0 M KOH solution.

Catalyst	η_j=10 mA cm^{-2} （mV）	Tafel slope (mV dec^{-1})	Reference
Ru@S, N-CMFs	**18**	**23**	**This work**
Ru/EG-rGO NCs	54	35	*ACS Catal.***2024**,14, 5416−5428
Ru/NC	21.9	29.03	*Adv. Funct. Mater.* **2023**, 2314899.
Ru/NCDs	37	25	*Small Methods*, **2022**, 6, 2200637
Ru-E-MXene/rGA	42	36.6	*Adv. Sci.* **2024**, 11, 2310013
Ru_{NP}-Ru_{SA}@CFN-800	33	37.16	*Adv. Funct. Mater.*, **2023**, 33, 2213058
Ru@SC-CDs 2:10	34	57	*Nano Energy*, **2019,** 65, 104023
Ru@CDs	30	22	*Small*, **2021**, 17, 2102496
S-Ru/C	54	31.08	*Appl. Catal. B Environ.*, **2023**, 335, 122896
NCAG/Ru-2	40	56.7	*Chem. Eng. J.*, **2022**, 442, 136337
Ru/NDC-4	28.5	20.8	*Appl. Catal. B Environ.*, **2023**, 327, 122466
Ru NPs-1.38	27	29	*ACS Catal.* **2023**, 13, 20, 13638–13649
hcp-Ru@NC-700	27.5	37	*ACS Catal.*, **2018**, 8, 7, 5714–5720
Ru_d= 7.0 Å	37	27	*Adv. Mater.*,**2024**, 36, 2310699.
Ru_{SA+NP}/DC	18.8	35.8	*Adv. Sci.*, **2021**, 8, 2004516
Ru/d-NPC	23	38	*Appl. Catal. B Environ.*, **2022**, 306, 121095
Ru/NC-400	39	49	*Adv. Funct. Mater.*, **2021**, 31, 2100698
Ru/C-H_2O/CH_3CH_2OH	35	36.2	*Appl. Catal. B Environ.*, **2019**, 258, 117
Ru@CN-0.16	32	64	*Energy Environ. Sci.*, **2018**, 11, 800-806

Table S3. Comparison of overall water splitting performance of Ru@S, N-CMFs with some previously reported Ru-based catalysts in 1.0 M KOH solution.

Catalyst	Overall voltage at 10 mA cm^{-2} (V)	Durability (h)	Reference
Ru@S, N-CMFs	**1.5**	**28**	**This work**
RuCo/Cu_2O/CF	1.56	24	*J. Chem. Phys.* 162, 244702 (**2025**)
Ru/RuO_2-NbB_2-v	1.55	15	*Fuel* 399 (**2025**) 135624
Ru@N-CNS	1.56	27	*Chem. Eur. J.* **2025**, 31, e202500651
Ru-MoO_2-Ni_3Mo_3N@NC	1.57	20	*Applied Catalysis B: Environmental* 278(**2020**)119281
HP-Ru/C	1.50	20	*Applied Catalysis B: Environmental* 294 (**2021**) 120230
Ru/NiFe LDH/NF	1.53	28	*Nanoscale*,**2020**,12, 9669-9679
Ru/$Co(OH)_2$ NWAs	1.54	25	*International Journal of Hydrogen Energy* 51 (**2024**) 769e776
Ru_1Co_2 NPs	1.59	10	*ACS Appl. Energy Mater.* **2020**,3,1869-1874
$SrFe_{0.7}Ru_{0.3}O_{3-\delta}$	1.58	24	*Applied Surface Science* 664 (**2024**) 160278
Ru-CoP/NC	1.58	20	*ACS Appl. Mater. Interfaces* **2021**, 13, 56035-56044

Table S4. Comparison of performance of Ru@S, N-CMFs with some previously reported Ru-based catalysts for AEMWE.

Catalyst	Stability (h)	Reference
Ru@S, N-CMFs	**246**	**This work**
c-$Ru_2(P_{0.9}Se_{0.1})$ DWNT/C	200	*Small Sci.* **2025**, 5, 2400610
NiRu/C (10 wt.% Ru)	100	*Small Methods* **2025**, 9, 2401179
$RuNi/MoO_2$	140	*Adv. Sci.* **2025**, 12, 2414622
Ru/NC-10	180	*Adv. Sci.* **2025**, 12, 2414012
Ni/NiO@Ru-NC	50	*ACS Nano* **2024**,18,1204-1213
Ru-NiCr/CP	24	*Chemical Engineering Journal* 514 (**2025**)
Ru_3Ni-N-C	200	*Energy Environ. Sci.*, **2025**, 18, 6273-6282
Ru-GaSA/N-C	170	*Nat Commun,* **2024**, 15, 6741.
np/Pt_1Ru_1-$Ni_{0.85}Se$	100	*Small* **2024**, 20, 2311178.
GaSA-Ru/RuO_2	200	*Adv. Funct. Mater.* **2025**, 35, 2503701.